PHYSICAL REVIEW B **79**, 121303(R) (2009)

Magneto-optical spectroscopy of excitons and trions in charge-tunable quantum dots

H. Sanada, T. Sogawa, H. Gotoh, Y. Tokura, H. Yamaguchi, H. Nakano, and H. Kamada
NTT Basic Research Laboratories, NTT Corporation, 3-1 Morinosato-Wakamiya, Atsugi-shi, Kanagawa 243-0198, Japan
(Received 5 December 2008; revised manuscript received 4 February 2009; published 6 March 2009)

We investigated the magneto-optical properties of charge-tunable GaAs quantum dots (QDs). Photoluminescence (PL) spectra change greatly with charge states of the QDs, and the PL lines of excited trions show complex magnetic field dependencies, which are quite different from that of the lowest radiative trion. A simulation using the configuration-interaction method supports the assignment of the PL emissions, and the effects of electron-electron and electron-hole interactions on shell and spin configurations of excited trions are discussed.

DOI: 10.1103/PhysRevB.79.121303 PACS number(s): 78.67.Hc, 71.35.Pq, 71.35.Ji

Spin states in semiconductor nanostructures are expected to act as quantum information carriers in solid-state systems.[1–3] One approach that allows us to access each spin is to use negative trions, which are composed of two electrons and one hole, in semiconductor quantum dots (QDs). An optically active trion in a QD serves as an intermediary for the initialization[4,5] and readout[6,7] of single-electron spin, using the optical selection rule that critically depends on the spin states of the trion and the resident electron. Because the spin properties of trions are characterized by the shell and spin configurations of the constituent electrons and a hole, Coulomb and exchange interactions and resultant energy structures are of particular interest.

Several optical spectroscopy techniques such as microphotoluminescence on single QDs, time- and polarization-resolved spectroscopies, and those employing electrically charge-tunable structures have supported the assignment of different charge states of QDs and enabled detailed studies of each of these states to be undertaken. Most experimental studies have, however, focused on their *lowest* radiative states, although a few recent reports have shown photoluminescence (PL) emissions related to *excited* states of trions: the PL of charged biexcitons (XX^-),[8–10] the polarized fine structure in PL excitation (PLE) spectra,[11] and the quantum beats in PL emissions from an ensemble of excited trions[12] have been reported. While the lowest state of the trion has all its electrons and its hole in ground shells (*s* shells), the excited trion has more than one electron or hole that occupies higher shells. These excited states mutually interact via Coulomb and exchange interactions, giving a rich variety of configurations. Furthermore, the carrier correlations in such excited states strongly depend on the external magnetic field, which in turn induces shell- and spin-dependent changes in energy and oscillator strength. In this respect, the spectrum of the trion excited states, which continuously evolves with increasing magnetic field, will provide an efficient way to assign the configurations in QDs.

In this study, we investigate the magneto-PL properties of a charge-tunable QD. We detected PL emissions from the excited radiative states as well as the lowest-lying state, probably because of partial spin blocking that may slow down the nonradiative energy relaxation. These emissions allowed us to overview their energy and oscillator strengths as functions of the magnetic field. Our experimental results and simulation using the configuration-interaction (CI) method reveal the roles of the direct Coulomb and exchange interactions and their effects induced via off-diagonal contributions to the excited trions in the QD.

Our sample consists of a 2.8-nm-thick GaAs single quantum well (QW) embedded in an *n-i*-Schottky diode grown on an *n*-GaAs substrate by molecular beam epitaxy [Fig. 1(a)]. A single electron, a neutral exciton, and a negative trion are created by tuning the bias voltage and/or by photoexcitation, all of which are confined within a potential minimum corresponding to a monolayer-thick island in the QW introduced by the growth interruption technique.[13] The lateral extent of the resulting QDs is estimated to be several tens of nanometers and their density is about 10^9 cm^{-2}. A Au/Ti film with small apertures of 0.25×0.25 μm^2 processed on top of the sample was used for area-selective spectroscopy of individual QDs and was also used as an electrode for applying a bias voltage between the surface and the substrate.

For micro-PL measurements, the sample was cooled to 6 K in a helium gas-flow cryostat placed in a superconducting magnet. A Ti:sapphire laser with a power density of about 10 W/cm^2 excited QDs within an aperture in the metal mask/electrode. The collected PL was then dispersed in a triple-grating monochromator and detected with a cooled charge-coupled device array. For magneto-PL measurements,

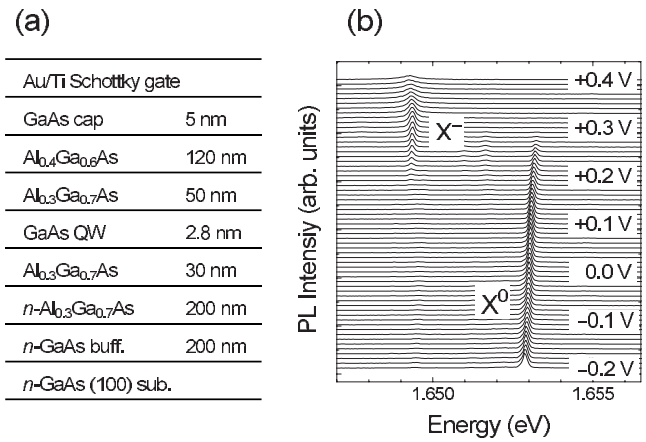

FIG. 1. (a) Sample structure. (b) PL spectra obtained in a bias range of $-0.2<V_g<+0.4$ V at $B=0$. The excitation energy was set to 1.6986 eV. The PL lines labeled X^0 and X^- are assigned to the lowest-lying neutral exciton and trion emissions, respectively.

an external magnetic field B was applied to the sample in the Faraday geometry and circular polarizations of the excitation and the PL were independently controlled with sets of polarizers and retarders.

Figure 1(b) shows typical PL spectra obtained in a bias voltage (V_g) range of $-0.2 < V_g < +0.4$ V at $B=0$. The PL line labeled X^0 (X^-) that appears as $V_g < 0.25$ V ($V_g > 0.25$ V) is assigned to the lowest-lying neutral exciton (negative trion). The energy of the X^- line is 3.8 meV lower than that of the X^0 line, which is consistent with previously reported values.[14,15] Further support to these assignments is obtained from linear-polarization-resolved PL spectra (not shown), where a fine energy splitting of about 30 μeV due to the anisotropic e-h exchange interaction is visible for X^0, whereas X^- shows no detectable splitting. The lowest-lying trion, which has two s-shell electrons, is known to show no energy splitting because the two electron spins are paired off.[16,17] Thus, the spectra shown in Fig. 1(b) are specific to the lowest exciton and trion emissions in axially asymmetric QDs.

The application of a magnetic field B provides us additional information about the carrier correlations and spin properties of excitons and trions in QDs. The color-scale plot in Figs. 2(a)–2(c) shows the B evolution of the polarization-resolved PL spectra at $V_g=0$, 0.25, and 0.3 V, respectively. The polarization of the excitation was switched between σ^+ and σ^- and the PL with the same polarization was detected.[18] The lowest-lying exciton (X^0) and the trion (X^-) emissions exhibit a diamagnetic shift with increasing $|B|$ and the corresponding coefficients are obtained as $\gamma(X^0)=18.7\pm1.0$ and $\gamma(X^-)=13.0\pm1.1$ μeV/T^2, respectively. The fairly large difference in γ reflects the substantial difference in the e-e or e-h correlation energy of the excitons and trions. We also found a small Zeeman splitting between two peaks with opposite polarizations shown as red and blue lines, which increased linearly with increasing $|B|$. The obtained effective g factors are $g(X^0)=1.18\pm0.06$ and $g(X^-)=1.29\pm0.08$. Their magnitudes are similar because they are determined by the difference between the g factors of the electron and hole. In addition to the lowest-lying exciton and trion emissions, we found several PL lines (labeled A, B, C, and D) at $V_g=0.25$ and 0.30 V [Figs. 2(b) and 2(c)], most of which exhibit much more complex B dependencies. [We also found line E, which is too weak to be recognized in Fig. 2. It will be discussed later with the enhanced graph that is shown in Fig. 4(f).] The most noteworthy is line A, whose energy decreases as $|B|$ increases. This huge decrease, which happens for both polarizations, is probably associated with the nonzero angular momentum of the electron or hole envelope function. Lines B and C also clearly deviate from simple parabola, and the intensity of line C decreases continuously with increases in $|B|$. For a more strongly charged condition at $V_g=0.3$ V [Fig. 2(c)], we find an additional parabolic line 2 meV below the X^- line (labeled D) and weak PL lines similar to A, B, and C at 0.25 V (but B dependencies are not exactly the same). We thus tentatively attribute these lines to some of the excited states of the negative trion.

For the excited-state PL emissions to be observed, the excited states need to retain small but nonvanishing populations within a time interval of the energy relaxation time. A previous report has shown that the energy relaxation rate of excited states via exciton-acoustic phonon interaction is 19 ps.[19] If we assume that the recombination lifetime of excited trions is the same order as that of ground excitons which has been reported as 100–230 ps,[20] we can observe the luminescence from the excited trion with the intensity 1 order of magnitude weaker than the ground-state emission.

We next consider the spin states of two electrons and one hole. If we assume a pseudospin approximation and no interaction between different configurations, the basic structures are determined by the requirement of Pauli's exclusion principle, in which two electrons act as two indistinguishable fermions.[21] For the ground state, we have two electrons in an s shell that form a spin singlet ($\uparrow_s\downarrow_s-\downarrow_s\uparrow_s$). For the excited states, on the other hand, two electrons reside in different shells (e.g., s and p shells) and could form both spin-singlet and -triplet ($\uparrow_s\uparrow_p$, $\uparrow_s\downarrow_p+\downarrow_s\uparrow_p$, and $\downarrow_s\downarrow_p$). These singlet and triplet are separated by an amount equal to the e-e exchange energy. Furthermore the isotropic e-h exchange interaction splits the triplet into three Kramers doublets at $B=0$ T.

This simple picture of basic spin configurations gives us additional hints to understand emissions of excited trions. Optically active excited states $\uparrow_s\uparrow_p\Downarrow$ or $\downarrow_s\downarrow_p\Uparrow$, in which two electrons in different shells have the same spin direction, require a spin flip in order to relax to a ground singlet $(\uparrow_s\downarrow_s-\downarrow_s\uparrow_s)\Downarrow$ or $(\uparrow_s\downarrow_s-\downarrow_s\uparrow_s)\Uparrow$. The energy relaxation rate governed by the spin-flip rate is slow enough to compete with that of spontaneous photon emission. As a result, PL from the excited states can be more intense.

It is not easy to identify the reason why the intensities of PL lines from the excited trions (lines A–D) vary between 0.25 and 0.30 V. We may point out that the phenomenon is causally related to (i) the excitation energy that possibly causes V_g-dependent absorbing level energy shifts due to the change in longitudinal QW potential, (ii) the electron tunneling rate that changes with internal electric field,[22] and (iii) the trion formation process, which does not always proceed with initial electron occupation (in the ground shell) followed by light-induced e-h creation; it also proceeds with e-h creation (in excited shells) and subsequent electron capture.[23] At present, however, such relevance and their interplay are unclear; thus, we need further an experiment to elucidate the mechanism of V_g-dependent excited trion emissions.

Figure 3(a) shows the schematic representation of the trion and electron energy levels and radiative transitions. The expression $(e_1e_2)_{t(s)}h$ describes the main part of shell configurations with two electrons (e_1e_2) and a hole (h) and subscript $t(s)$ represents spin-triplet (-singlet) states of two electrons. The excited states are split into singlet and triplet, and the triplets are split into two bright (solid lines) and one dark (dashed lines) levels. The ordering of the levels is determined by e-e and e-h interactions, which depend on B. In addition, because the interaction energies are the same order of magnitude as the kinetic energies, they are given as generalized Coulomb matrix elements represented by $\langle i,j|V_{e\text{-}e(e\text{-}h)}|k,l\rangle$ for e-e (e-h) scattering in a basis of Slater determinants constructed from all possible shell and spin occupations. This introduces off-diagonal as well as diagonal elements in the Hamiltonian, and as a result, different configurations mix.

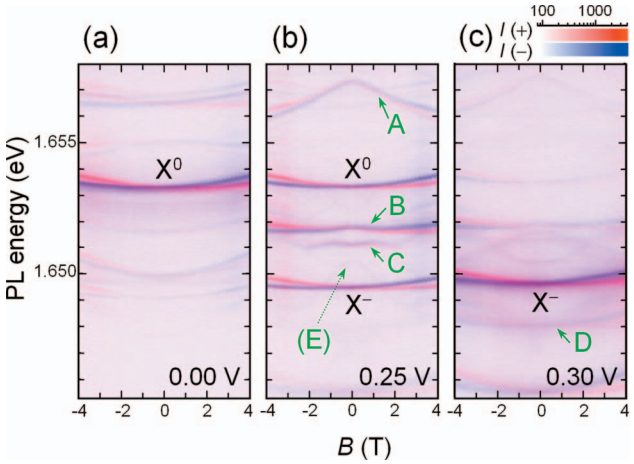

FIG. 2. (Color) Magnetic field evolution of the polarization-resolved PL spectra at bias voltages of (a) 0, (b) 0.25, and (c) 0.3 V. The density plots of the logarithm of the intensity for σ^+ (expressed by depth of red) and σ^- excitations (blue) overlap in each graph. The excitation energy was set to 1.6750 eV.

To understand trion configurations in a magnetic field qualitatively in more detail, we carried out a CI calculation. We model the QD confinement with a two-dimensional parabolic potential $U_{e(h)}(x,y)=m_{e(h)}(\omega^2_{e(h),x}x^2+\omega^2_{e(h),y}y^2)/2$. When the QD potential is axially symmetric $(\omega_{e(h),x}=\omega_{e(h),y})$, single-particle energies and envelope functions are of well-known Fock-Darwin states.[24,25] In actual QDs, however, the symmetry is reduced $(\omega_{e(h),x}\neq\omega_{e(h),y})$. Thus we used the eigenfunctions for the elliptic QDs derived by analytical procedures.[26,27] In the simulation, we considered parameters ω_0 and $\delta\omega$, which gave $\omega_{e,x(y)}=m_h/(m_e+m_h)(\omega_0\pm\delta\omega)$ and $\omega_{h,x(y)}=m_e/(m_e+m_h)(\omega_0\pm\delta\omega)$, keeping the symmetry $m_e\omega_{e,x(y)}=m_h\omega_{h,x(y)}$.[28] We took account of the shells of the electron and hole up to the d shell and disregarded the Zeeman splittings and anisotropic parts of the e-h exchange interactions for simplicity. The diagonal and the off-diagonal e-e and e-h Coulomb matrix elements were obtained by numerical integration.[27]

The electron and trion energies as a function of B are shown in the bottom and top graphs in Fig. 3(b), respectively. For the electron, we name the shells $s, p_\pm, d_{0,\pm}$ for the following discussion. As seen in the graph for the trion, as the energy increases, the states become more crowded. We mainly focus on the six types of configuration from the lowest as indicated by the arrows in Fig. 3(b).

From the obtained eigenstates and energies we can calculate the oscillator strength for a given set of initial and final states, which are the mixture of several configurations.[28] This is calculated according to Fermi's golden rule, $I(\omega)=|\langle\Psi_f|\hat{P}^\pm|\Psi_i\rangle|^2\delta(E_i-E_f-\hbar\omega)$, where subscript i (f) represents the initial trion (final electron) state, respectively. The interband polarization operator $\hat{P}_\pm$ for $\sigma^\pm$ polarization is given by $\hat{P}_\pm=\Sigma_j(\hat{b}_{j,\mp1/2}\,\hat{a}_{j,\mp1/2})$, where $\hat{a}_{j,\mp1/2}$ $(\hat{b}_{j,\mp1/2})$ is an

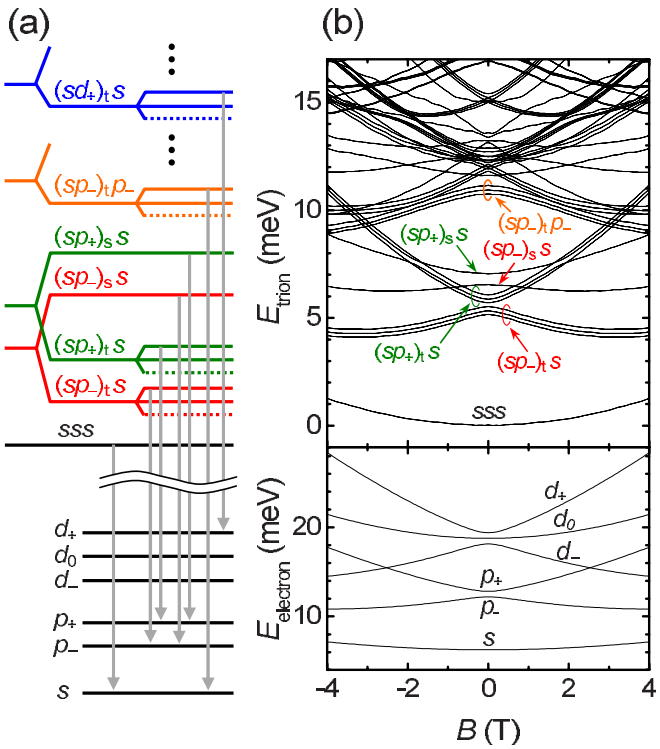

FIG. 3. (Color online) (a) Energy diagram for a single electron and a negative trion at $B=0$ T. Labels s and t denote the singlet and triplet configurations for two electrons. (b) Calculated total energy vs B. The parameters are assumed as $m_e=0.067$, $m_h=0.112$, $\hbar\omega_0=10$ meV, $\hbar(\delta\omega)=0.5$ meV, and $\Delta_0=0.4$ meV.

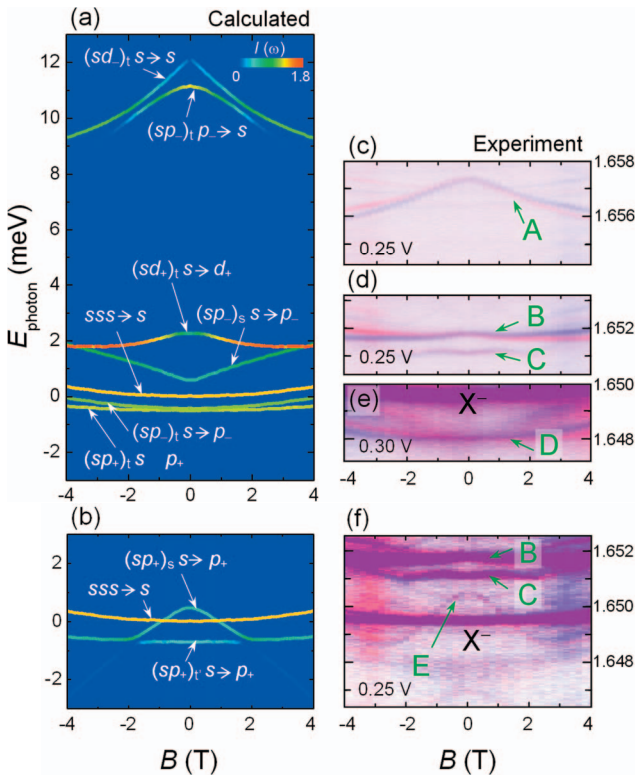

FIG. 4. (Color) (a) Density plot of calculated oscillator strength as a function of photon energy E_{photon} and B for several transitions. E_{photon} is offset so that the energy for $sss\rightarrow s$ at $B=0$ T becomes 0 meV. Some other transitions are plotted in (b). (c)–(f) Parts of the experimental data are replotted from Fig. 2 for comparison. Enhanced color is used for weak signals in (e) and (f).

annihilation operator that removes the electron (hole) in the jth shell with a pseudospin of $\mp 1/2$. Several calculated spectra are displayed in Figs. 4(a) and 4(b) as functions of B, where the oscillator strengths are represented by the density of the lines.

Now we compare the simulated results and the experimental data shown in Figs. 4(c)–4(f). For the radiative excited triplet ($\uparrow\uparrow\Downarrow$ or $\downarrow\downarrow\Uparrow$), we consider the following three transitions: in the simulation [Fig. 4(a)], the transition $(sp_-)_t p_- \rightarrow s$, which shifts to a lower energy with increasing $|B|$, reproduces the experimentally obtained line A until it anticrosses with the $(sd_-)_t s \rightarrow s$ line at $B \approx \pm 1.5$ T. The transitions $(sp_\pm)_t s \rightarrow p_\pm$, which are located at an energy lower than $sss \rightarrow s$, well explain the observed PL line D. We also plot $(sd_+)_t s \rightarrow d_+$ as the transition that is close to line B.

For the excited singlet $[(\uparrow\downarrow - \downarrow\uparrow)\Uparrow$ or $(\uparrow\downarrow - \downarrow\uparrow)\Downarrow]$, $(sp_-)_s s \rightarrow p_-$ is one of the possible assignments for the PL line C, which appears as $|B| \lesssim 2$ T, although there still exists discrepancy in their B dependencies. Furthermore this assignment requires a mechanism for the suppressed energy relaxation that depends on B, e.g., the phonon bottleneck effect in QDs.[29] When we again focus on the enhanced data at $V_g = 0.25$ V in Fig. 4(f), we notice a weak line E that traces the simulated transition $(sp_+)_s s \rightarrow p_+$ in Fig. 4(b) and there may be singlet-triplet anticrosses at $B \approx \pm 2$ T. As seen above, although there are still numerical discrepancies, the model can explain large parts of our experimental PL spectra qualitatively.

Finally we remark on the generality of the observed phenomena. We have investigated another QD that has similar PL lines that emit from an excited trion, but the B dependence is not exactly the same: although we can find lines corresponding to lines A, B, and C with similar energy structures as above, the intensity of line B disappears rather than that of line C as $|B|$ increases. We tentatively attribute this to the carrier correlation, which is sensitive to the QD potential or other factors. In fact, in the present sample, the B dependence of line C varies with V_g [Figs. 2(b) and 2(c)]. This is probably because the ratio of the e-e and e-h interactions, which is set to 1 in the simulation, is affected by an electric field induced by V_g.

In conclusion, we have observed PL emissions from a single exciton and a negative trion in a charge-tunable QD. The PL spectra change greatly with the charge states of the QDs, and the PL lines of excited trions show complex magnetic field dependencies, which are quite different from that of the lowest radiative trion. From a simulation using the elliptic Fock-Darwin model, we speculated on the origin of the trion PL emissions, in which off-diagonal elements of the e-e and e-h interactions have significant roles to determine the shell and spin configurations in the trion system. We believe that the present work opens the possibility of developing a scheme for the optical control of single-electron spins using the excited states of trions in QDs.

We thank T. Tawara, G. Zhang, and A. Matsudaira for useful discussions. We also thank M. Ueki for technical support with the sample preparation. This work was partly supported by the Japan Society for the Promotion of Science (JSPS).

[1] A. Imamoglu, D. D. Awschalom, G. Burkard, D. P. Di Vincenzo, D. Loss, M. Sherwin, and A. Small, Phys. Rev. Lett. **83**, 4204 (1999).
[2] F. H. L. Koppens *et al.*, Nature (London) **442**, 766 (2006).
[3] D. Press *et al.*, Nature (London) **456**, 218 (2008).
[4] M. Atatüre, J. Dreiser, A. Badolato, A. Högele, K. Karrai and A. Imamoglu, Science **312**, 551 (2006).
[5] X. Xu, Y. Wu, B. Sun, Q. Huang, J. Cheng, D. G. Steel, A. S. Bracker, D. Gammon, C. Emary, and L. J. Sham, Phys. Rev. Lett. **99**, 097401 (2007).
[6] J. Berezovsky *et al.*, Science **314**, 1916 (2006).
[7] M. Atatüre, J. Dreiser, A. Badolato and A. Imamoglu, Nat. Phys. **3**, 101 (2007).
[8] I. A. Akimov *et al.*, Appl. Phys. Lett. **81**, 4730 (2002).
[9] I. A. Akimov, K. V. Kavokin, A. Hundt, and F. Henneberger, Phys. Rev. B **71**, 075326 (2005).
[10] N. I. Cade, H. Gotoh, H. Kamada, H. Nakano, and H. Okamoto, Phys. Rev. B **73**, 115322 (2006).
[11] M. E. Ware, E. A. Stinaff, D. Gammon, M. F. Doty, A. S. Bracker, D. Gershoni, V. L. Korenev, Ş. C. Bădescu, Y. Lyanda-Geller, and T. L. Reinecke, Phys. Rev. Lett. **95**, 177403 (2005).
[12] I. E. Kozin, V. G. Davydov, I. V. Ignatiev, A. V. Kavokin, K. V. Kavokin, G. Malpuech, H. W. Ren, M. Sugisaki, S. Sugou, and Y. Masumoto, Phys. Rev. B **65**, 241312(R) (2002).
[13] D. Gammon, E. S. Snow, B. V. Shanabrook, D. S. Katzer, and D. Park, Phys. Rev. Lett. **76**, 3005 (1996).
[14] A. S. Bracker *et al.*, Phys. Rev. Lett. **94**, 047402 (2005).
[15] A. S. Bracker *et al.*, Phys. Rev. B **72**, 035332 (2005).
[16] M. Bayer *et al.*, Phys. Rev. B **65**, 195315 (2002).
[17] J. G. Tischler, A. S. Bracker, D. Gammon, and D. Park, Phys. Rev. B **66**, 081310(R) (2002).
[18] We have confirmed that the Overhauser shift is negligibly small such that <0.05 meV; thus, we safely neglect its relevance in the scope of the present work.
[19] D. Gammon, E. S. Snow, B. V. Shanabrook, D. S. Katzer, and D. Park, Science **273**, 87 (1996).
[20] J. Hours, P. Senellart, E. Peter, A. Cavanna, and J. Bloch, Phys. Rev. B **71**, 161306(R) (2005).
[21] K. V. Kavokin, Phys. Status Solidi A **195**, 592 (2003).
[22] S. Seidl *et al.*, Phys. Rev. B **72**, 195339 (2005).
[23] H. Sanada *et al.*, Phys. Status Solidi C **5**, 2904 (2008).
[24] V. Fock, Z. Phys. **47**, 446 (1928).
[25] C. G. Darwin, Proc. Camb. Philos. Soc. **27**, 86 (1931).
[26] O. Dippel, P. Schmelcher, and L. S. Cederbaum, Phys. Rev. A **49**, 4415 (1994).
[27] Y. Tokura, S. Sasaki, D. G. Austing, and S. Tarucha, Physica B **298**, 260 (2001).
[28] P. Hawrylak, Phys. Rev. B **60**, 5597 (1999).
[29] T. Fujisawa *et al.*, Nature (London) **419**, 278 (2002).